ISCI, Volume *21*

Supplemental Information

KDM3A and KDM4C Regulate Mesenchymal Stromal Cell Senescence and Bone Aging via Condensin-mediated Heterochromatin Reorganization

Biao Huang, Bin Wang, Wayne Yuk-Wai Lee, Kin Pong U, Kam Tong Leung, Xican Li, Zhenqing Liu, Rui Chen, Jia cheng Lin, Lai Ling Tsang, Baohua Liu, Ye chun Ruan, Hsiao Chang Chan, Gang Li, and Xiaohua Jiang

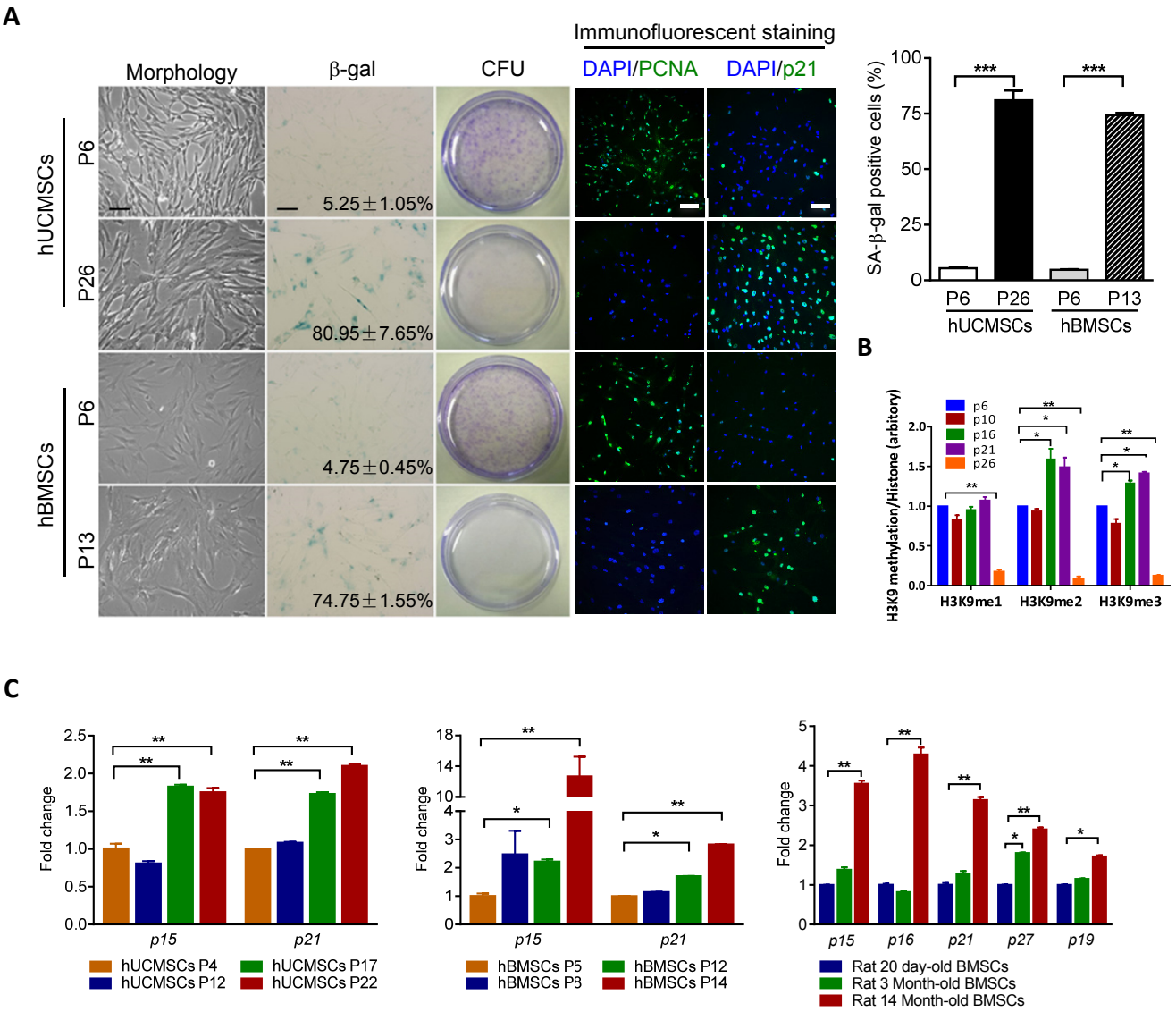

Supplementary Figure S1: Establishment of replicative senescence model using MSCs, Related to Figure 1

Three hUCMSCs lines (hUC009, hUC011, hUC013) and three hBMSCs lines (hBM001, hBM003, hBM005) were used for serial passaging, and characterized with various senescence markers. **(A)** Representative images of morphology, β-Gal staining, colony formation and immunofluorescence staining of PCNA and p21 (scale bar=100μm) in early passage hUCMSCs (p6) and hBMSCs (p6) compared with late passage hMSCs (p26 for hUCMSCs, p13 for hBMSCs). Quantification of β-Gal staining in early passage hUCMSCs and hBMSCs compared with late passage hMSCs. Data are presented as the mean ± SEM. ***p<0.001 (t test, n=3). **(B)** Quantification of protein expression of H3K9me, H3K9me2, H3K9me3 during MSC senescence as shown in Figure 1B. *p<0.05; **p<0.01(t test, n=3). **(C)** RT-qRCR analysis of cell cycle inhibitors in 3 senescence models. Data are presented as mean ± SEM. *p<0.05; **p<0.01 (t test, n=3). For Rat BMSCs, MSCs were isolated from the bone marrow of SD rats at different ages, (20 days, n=3; 3 months, n=3; 14 months, n=3).

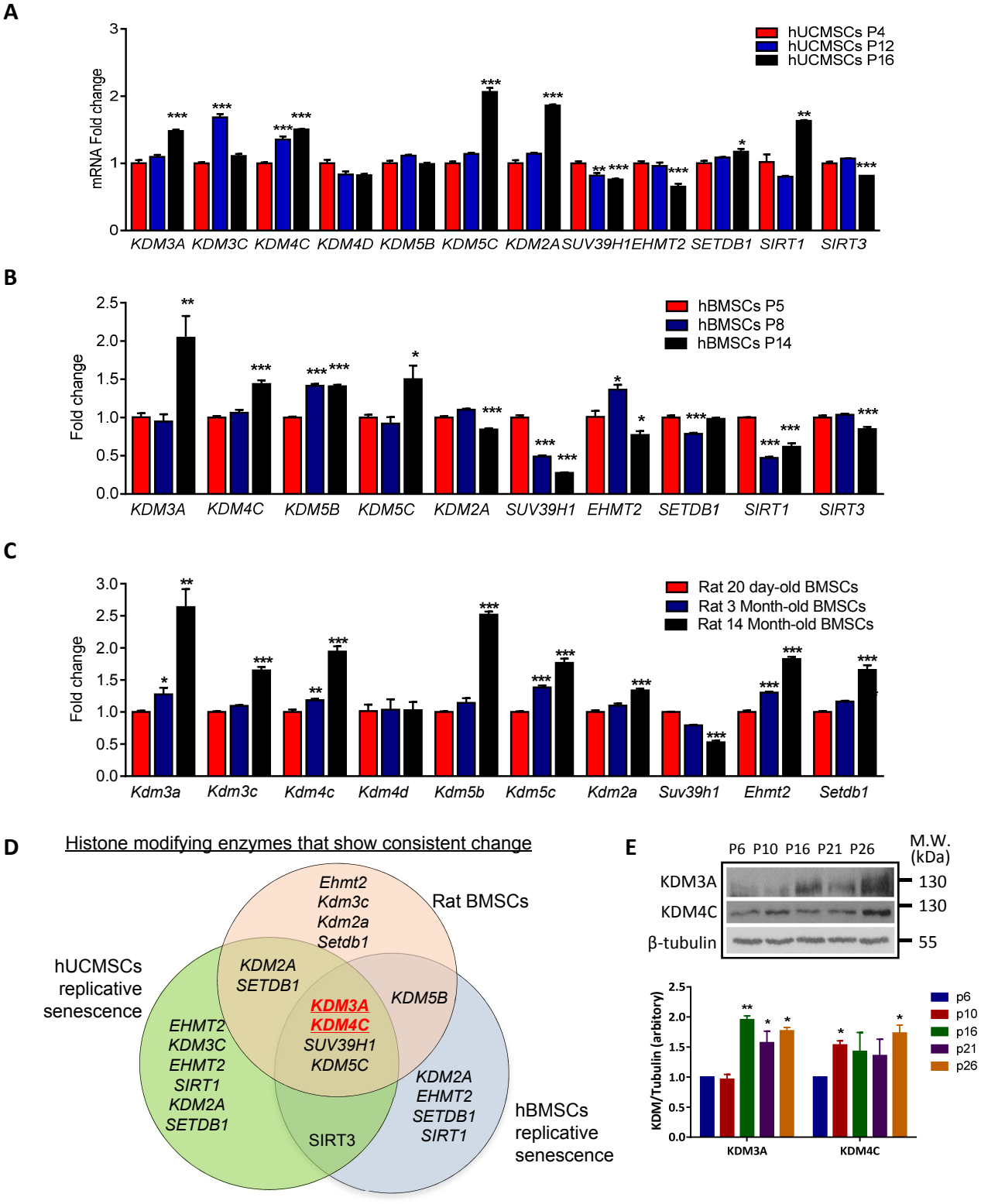

Supplementary Figure S2: Screening of histone-modifying enzymes involved in MSC senescence, Related to Figure 1
(A-C) Gene expression profiling of histone modifying enzymes in hUCMSCs replicative senescence model, hBMSCs replicative senescence model and primary rat BMSCs with physiological aging. Data are presented as the mean ± SEM. *p<0.05; **p<0.01;***p<0.001(t test n=3). **(D)** Venn diagram reveals the commonly differentially-expressed histone modifying enzymes in three senescence models. **(E)**Representative western blot showing the protein expression levels of KDM3A and KDM4C increase with hUCMSC aging. Experiments were repeated three times with two hUCMSCs lines, *p<0.05; **p<0.01 (t test, n=3).

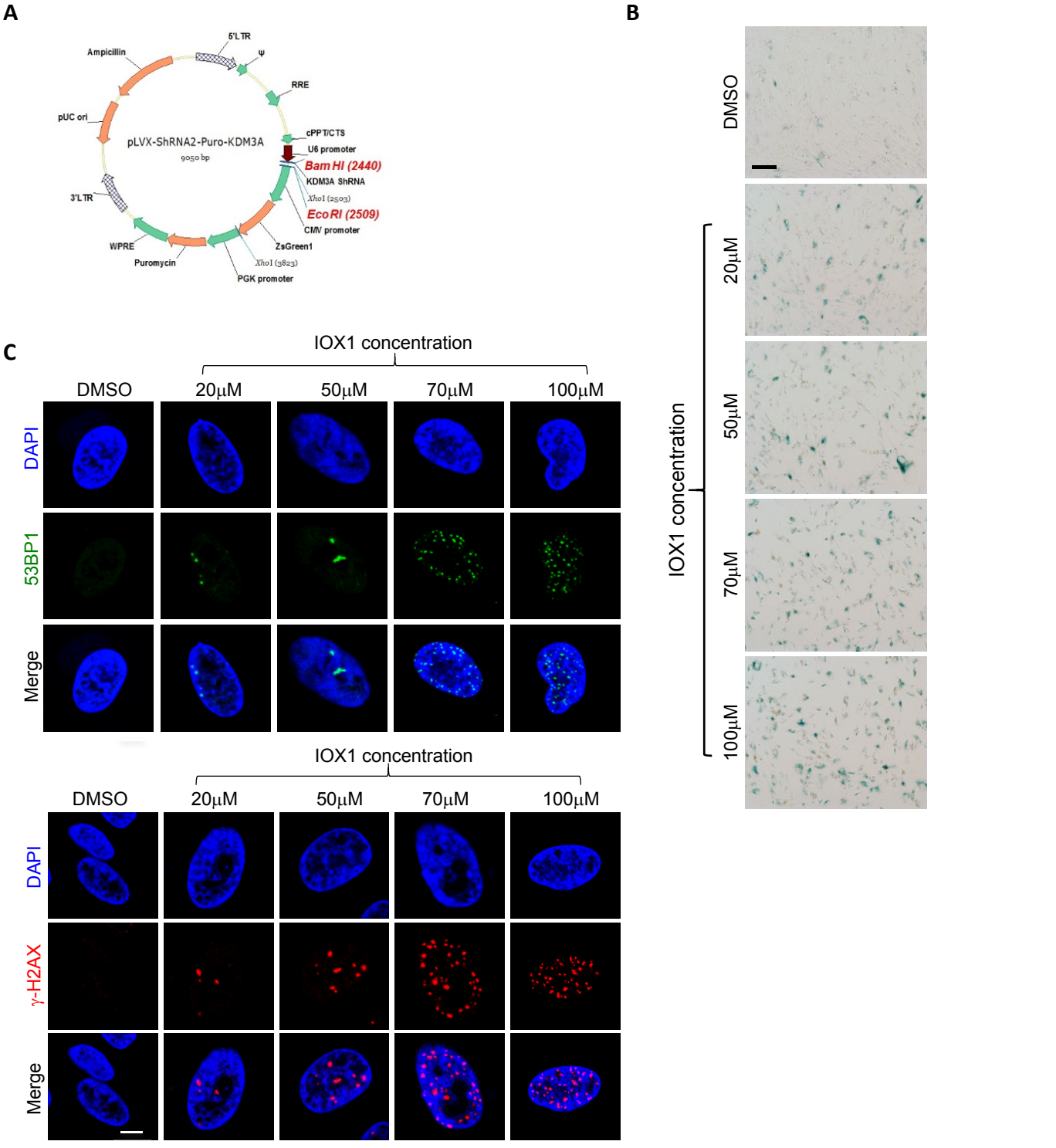

Supplementary Figure S3: KDM inhibitor IOX1 induces DNA damage and cellular senescence in MSCs, Related to Figure 2
(A) Map of lentiviral vector containing shRNA-KDM. **(B)** Representative images of β-Gal staining in hUCMSCs (p7) treated with different concentrations of IOX1 (scale bar=100μm). **(C)** Representative images of 53BP1 and γ-HA2X staining in hUCMSCs (p7) treated with different concentrations of IOX1 (scale bar=5μm).

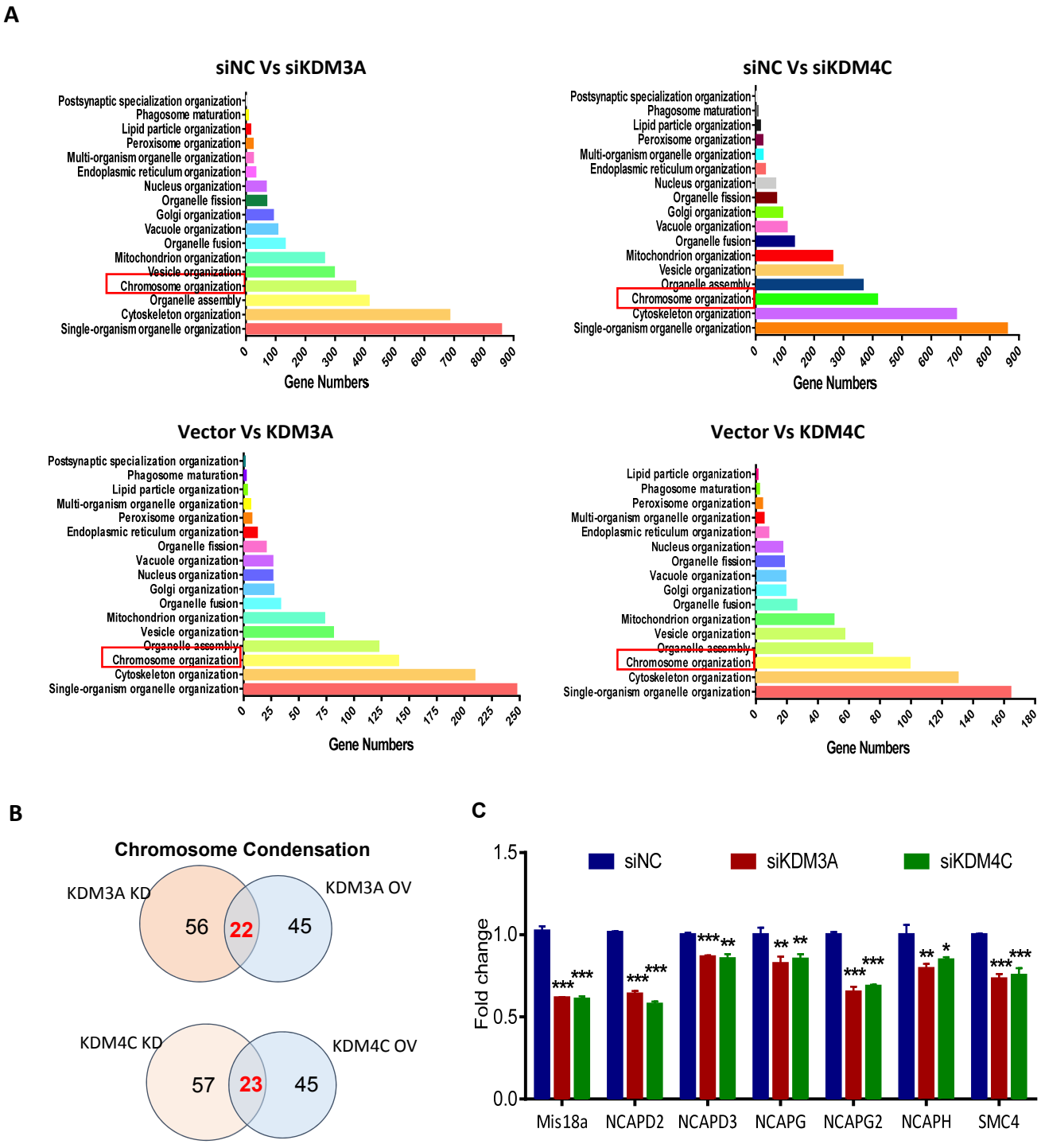

Supplementary Figure S4: KDM3A and KDM4C regulate chromosome condensation genes, Related to Figure 3
(A) GO analysis of differentially expressed genes (DEGs) on organelle organization based on RNA-Seq results comparing siKDM3A-1 or siKDM4C-3-treated hUCMSCs with Scrambled siRNA-treated hUCMSCs, or *KDM3A*- or *KDM4C*-overexpressing hUCMSCs with vector control-transfected hUCMSCs. **(B)** Venn diagram reveals the commonly differentially-expressed chromosome condensation genes in KD and overexpressing cells compared to their respective control cells. **(C)** RT-qPCR assay showing the expression levels of condensin subunits in siKDM3A-(siKDM3A-1+siKDM3A-3) or siKDM4C-(siKDM4C-1+siKDM4C-3) - or Scrambled siRNA-treated hUCMSCs. Data are presented as mean±SEM. *p<0.05; **p<0.01;***p<0.001 (test, n=3).

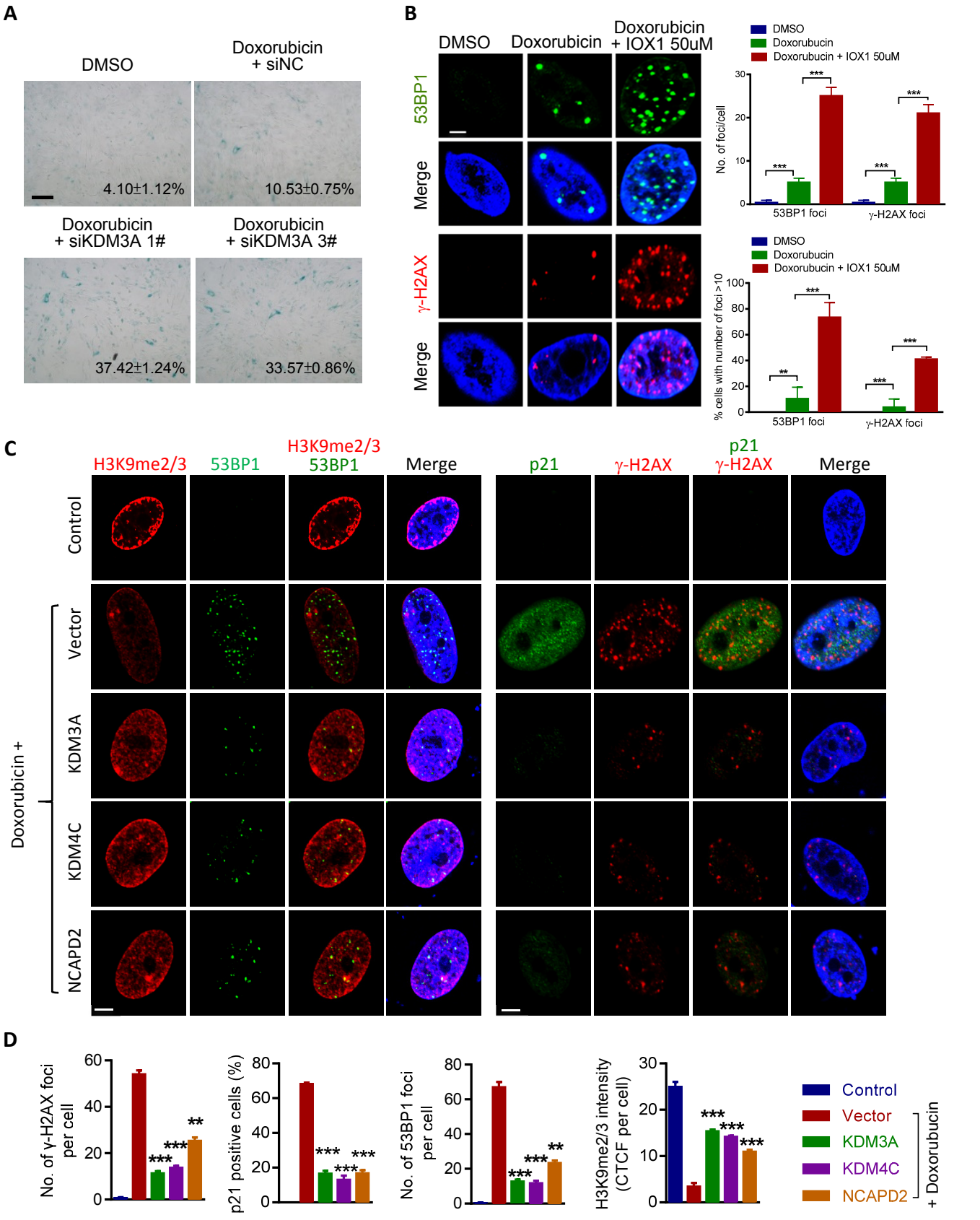

Supplementary Figure S5: KDM3A and KDM4C regulate DNA damage-induced senescence via NCAPD2, Related to Figure 4
(A) Representative images of β-Gal staining in Doxorubicin- treated hUCMSCs with Scrambled siRNAs or siKDM3A-1 or siKDM3A-3. (scale bar=100μm). **(B)** Representative images and quantification of 53BP1 and γ-H2AX immunofluorescence staining (scale bar=5μm) in hUCMSCs treated with Doxorubicin only or Doxorubicin + IOX1 50μM. mean±SEM of values from three different experiments with triplicate wells analyzed on 6-8 cells/field from five different fields ;***p<0.001 (t test). **(C-D)** Representative images and quantification of 53BP1, γ-H2AX, p21 and H3K9me2/3 immunofluorescence staining (scale bar=5μm) in control or Doxorubicin-treated hUCMSCs transfected with Vector plasmid or *KDM3A*, *KDM4C* or *NCAPD2* plasmid (CTCF, corrected total cell fluorescence). Mean±SEM of values from three different experiments with triplicate wells analyzed on 6-8 cells/field from five different fields. **p<0.01;***p<0.001 by t test compared to vector control treated with DOX.

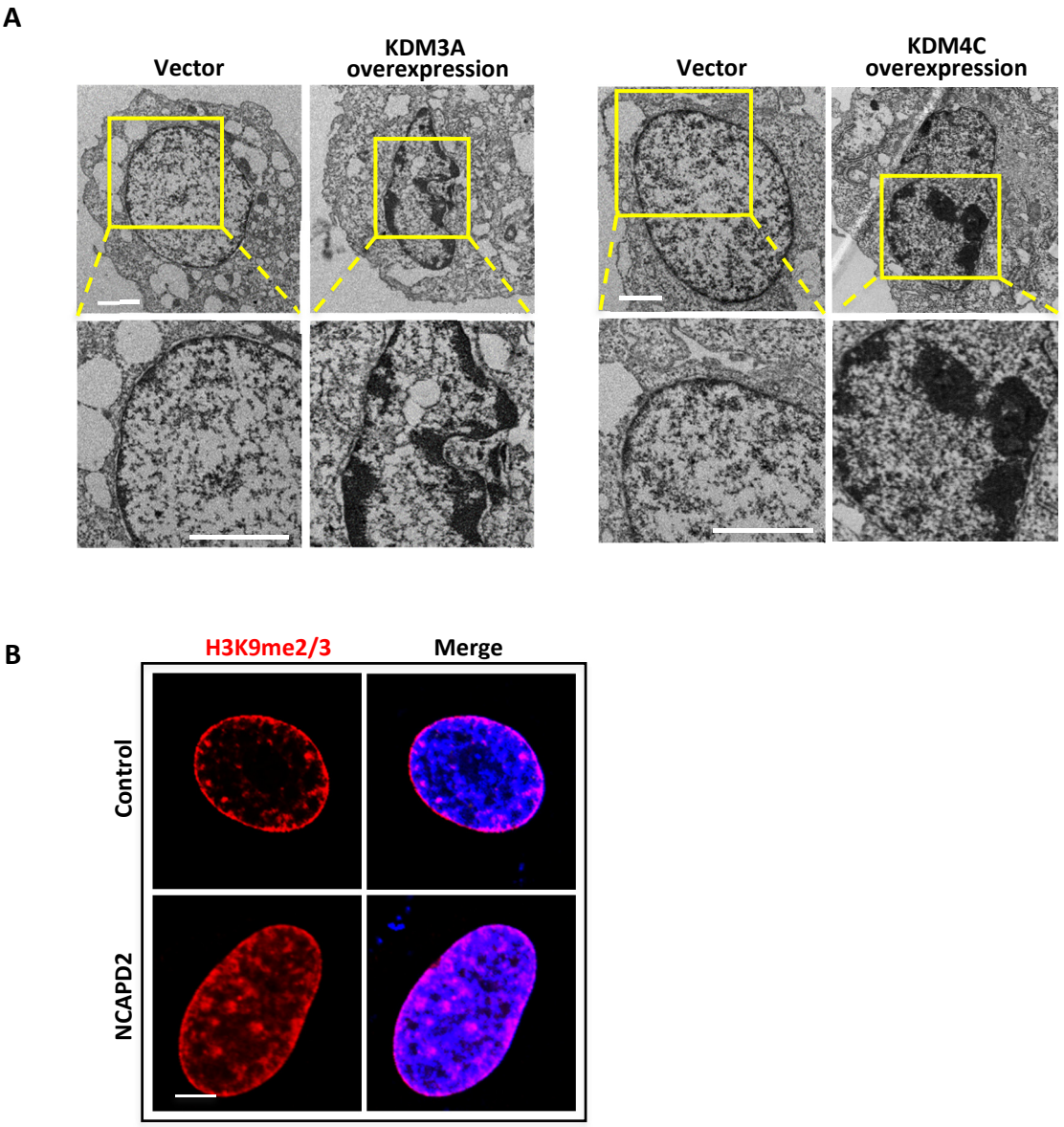

Supplementary Figure S6: KDM3A and KDM4C promote chromosome organization, Related to Figure 4
(A) Representative images of Transmission Electron Microscope (TEM) on the nucleus of hUCMSCs transfected with *KDM3A* or *KDM4C* or vector plasmid. The experiment was performed using hUC013. **(B)** Representative images showing overexpression of *NCAPD2* promotes formation of heterochromatin foci as demonstrated by H3K9me3 (red) staining (scale bar=5μm).

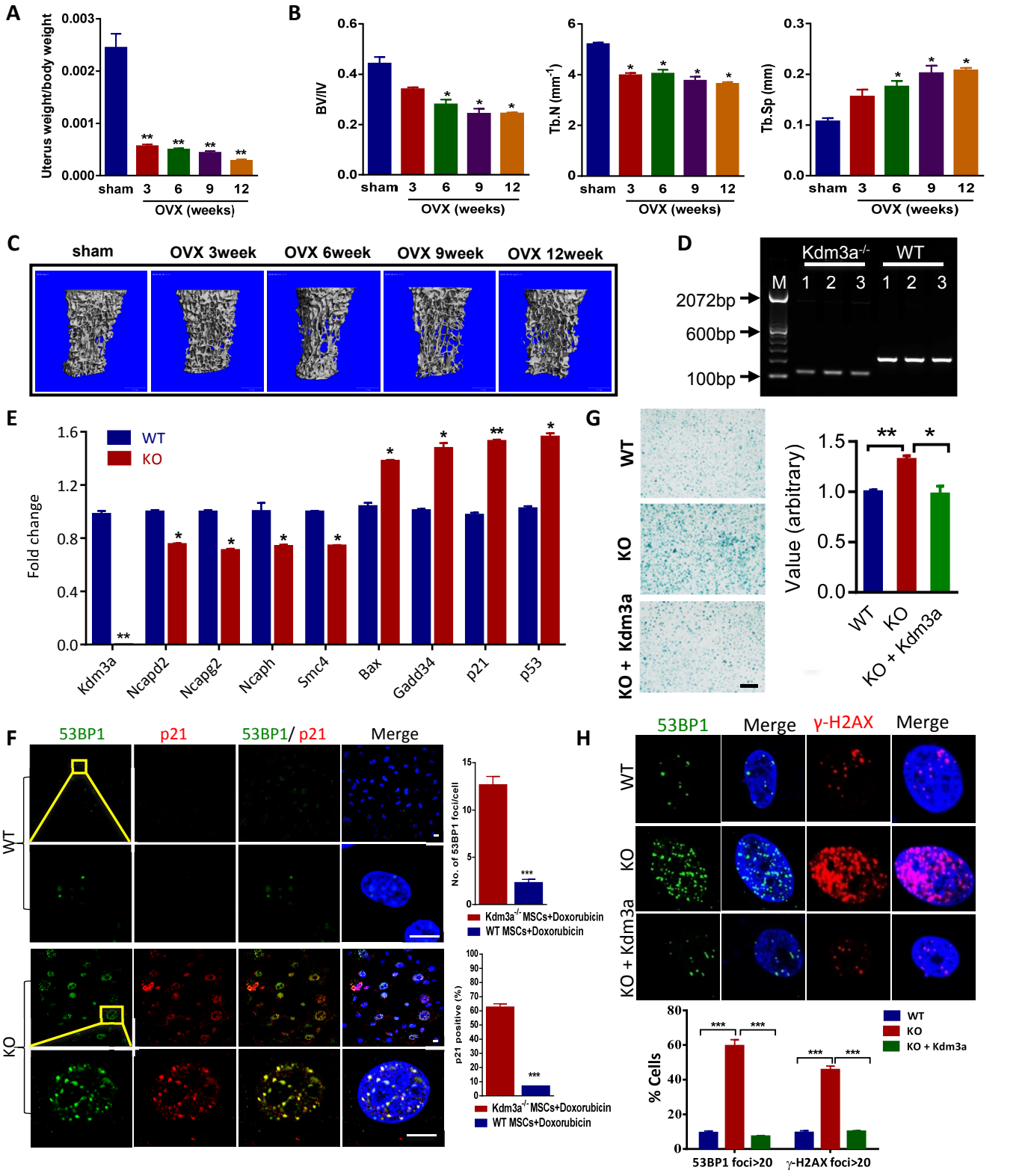

Supplementary Figure S7: Kdm3a affects bone aging *in vivo*, Related to Figure 5 and Figure 6

(A) Quantification data of uterus of sham and OVX-treated rats at 12 weeks (total n=29, sham group n=5, OVX 3weeks n=6, OVX 6weeks n=6, OVX 9weeks n=6, OVX 12weeks n=6). **p<0.01, (Wilcoxon/Mann-Whitney test). **(B)** The quantification of morphometric parameters including bone volume fraction (BV/TV), trabecular number (Tb.N, 1/mm) and trabecular separation (Tb.Sp, mm) in rat OVX rats. *p<0.05(Wilcoxon/Mann-Whitney test). **(C)** The representative three-dimensional reconstructed images of trabecular microarchitecture of 5th vertebral bodies in rat OVX rats. **(D)** Genotyping of WT and *Kdm3a* KO mice. **(E)** qPCR assay showing the downregulation of condensin components and upregulation of cell cycle regulators in BMSCs collected from 6 month-old *Kdm3a*$^{-/-}$ mice (n=3) compared to WT mice (n=3), *p<0.05;**p<0.01 (t test). **(F)** Representative images of immunofluorescence staining of p21 and 53BP1 in Doxorubicin (5 x 10^{-8} M)-treated BMSCs derived from 6 month-old *Kdm3a*$^{-/-}$ mice (n=3) and WT mice (n=3). Mean±SEM of values from three different experiments with triplicate wells analyzed on 6-8 cells/field from five different fields; ***p<0.001 (t test). **(G)** Representative images and quantification of β-Gal staining (scale bar=100μm) show KDM3A rescues Doxorubicin-induced cellular senescence in KO BMSCs. Each plate represents BMSCs derived from a single mouse, n=3 for each group. *p<0.05; **p<0.01 (t test). **(H)** Representative images and quantification of 53BP1 and γ-H2A.X immunofluorescence staining (scale bar=5μm). Overexpression of kdm3a in KO BMSCs completely rescues Doxorubicin-induced DNA damage (n=3). Data are presented as mean±SEM of values from three different experiments with triplicate wells analyzed on 6-8 cells/field from five different fields,***p<0.001 (t test).

Supplementary Table S1: Detailed information of BMSCs, Related to Figure 7

Inventory ID	Disease	Age	Gender	Race
BMMSC4 2009	Mild anemia	13	M	Asian
BMMSC5 2010	None	16	M	Asian
BMMSC7 2009	Mild anemia	17	M	Asian
BMMSC3 2009	None	21	M	Asian
BMMSCS04	None	26	M	Asian
BMMSCS01	None	27	M	Asian
BMMSCS006	None	30	M	Asian
BMMSCS05	None	32	M	Asian
BMMSCK009	None	25	M	Asian
BMMSCS005	None	61	M	Asian
BMMSC S007	None	52	M	Asian
BMMSC K006	None	55	M	Asian
BMMSC K005	None	54	M	Asian
BMMSC K008	None	57	M	Asian

Supplementary Table S2. Primers used in this study, Related to Figure 2, Figure 3, Figure 5 and Figure 6

Primers for qPCR (Human primers)

Target	Forward primer (5' to 3')	Reverse primer (5' to 3')
hKDM5A	TATCCCAAGCGACTACCCAC	TCCTGGATCTGTATGCTTTGA
hKDM5B	AGTTTGGGCCTCCAATTCAT	CGAGCAGACTGGCATCTGTA
hKDM5C	TTGTAGCCTTGGTTGAAGCC	ACCCTCATGAATCCCAACAC
hSIRT1	AGAGATGGCTGGAATTGTCC	CCAGATCCTCAAGCGATGTT
hSIRT3	AGAACACAATGTCGGGCTTC	CACAGTCTGCCAAAGACCCT
hEHMT2	GAGGTCACCTTTCCCAGTGA	AACCATGTCCAAACCAGGAA
hSETDB1	TTCACGGAGCTTCTGGTCTT	TTCCCGGCCTACAGAAATAA
hSUV39H1	ACACGTCCTCCACGTAGTCC	CAAGAACAGCTTCGTCATGG
hKDM4A	GGAGCTTGCTTAAAGGCTGA	GAAGCGCCGCTAGAAGTTT
hKDM4B	CGTCCATGGAGATCTTGACC	TTCAATCACGGGTTCAACTG
hKDM4C	TCACCATGTCTTTCCTGCAA	TTCCCATATGGCTACCATGC
hKDM4D	CCACATACCAAGTTTTGGGC	GTGGAAAACCACGTTTGCTT
hKDM3A	TTCTTTTCCTCCAAGATTCCC	GGGACCATTCGAGCTGTTT
hJMJD1C	AGTAAACCACTGGGTGGCAG	AGCCTTGTTGTGGATTTCTGA
hKDM2A	CCATCATCTTCATAGCGTCG	AGCCCTGGAGTGGTTTCTTT
hKDM2B	AGCTCCTGCCGTTGTCC	TGGCCAAAGAAGACTCCAAA
hKDM6B	CGCTGCCTCACCCATATCC	ATCCGCGACCTCTGAACTCT
hLMNB1	TCTTTCGAATTCAGTGCTGC	AAGTGCAAGGCGGAACAC
hCENPA	GTCTCCGCCGACTGTGTT	CCTCTGCGGCGTGTCAT
hH2AFZ	CTTTCCGGAGTCCTTTCCAG	GTGGGTCCGATTAGCCTTTT
hNCAPD2	GGCAGCCTGAAAAGCTCTAA	CCCCAGAGGAGTTGTTGAAA
hNCAPG2	AAATTCTTCAGCCTTTGCCAT	GCTGGTTGGAGAGTTTTTGC
hHJURP	CAAACAGAGAGCAAGTGGGA	TCTTCACAGCCCAACTCAGA
hMis18a	CAAGATTGAGTGAGCACCCC	ATCCTGCTTCGCTGTGTTTC

Primers for qPCR (Rat primers)

Target	Forward primer	Reverse primer
rKdm3a	TTGCTCTGAGGTCTCTCCCA	GCAGTACAGCCAAGCAGGAT
rJmjd1c	TGC GCT GAC CTT CAA ACC AT	GTT CGG GCT TTA GGC TGT CT
rKdm4c	TGG AGA GTC CCC TAA ATC CCA	TTG GCA AGA CCT GCT CGA TG
rKdm4d	AGGCGCAAATAAGTACGGGG	CGGGTGCAGCAGAATCTCTT
rKdm5b	GCC ACC ATT CGC TTG TGA TG	TTA CAC GTG TTT GGG CCT CC

rKdm5c	GGT TCC TTG CTA CGC TCT CA	TAC ACT GCA CAA GGT TGG CT
rKdm2a	GGCATCCGGGAGTGGTTTCT	TACCACGCAATCTCTGGCTG
rSuv39h1	GGCGCCACCTACCTCTTTGA	CGTTGTACACCTGCAGGTTG
rEhmt2	GAGCCGCCGAGAGAGTTC	GGTGTCAGCCCCCTCATC
rSetdb1	TTTGCAAAGTACTCATCACCCA	TTGGATGACATTGCTAAAGGCT
rSirt1	TCAAGGCTGTTGGTTCCAGT	AAGGCGTCATCTTCAGAGTC
rSirt3	GGCACTACAGGCCCAATGTC	TCTCTCAAGCCCGTCGATGT
rNcapd2	AATTGTGGGCAAACTGCGTC	CAGAGGCTGTTGCCTTGAGA
rNcapg2	TGCTTGAGTGCTGCTGTGTA	TGTGGCCTTGAGATACGACG
rCenpa	GGCACTACACAGAAGACGGA	CACACCACGGCTGAATTTCC
rHjurp	AGTCTGGGGAGGAAAGCTGA	AAGCTTGTATCTGCACCGCT
r p15/INK4b	TCACCAGACCTGTGCATGAT	AGGCGTCACACACATCCAG
r p16/INK4a	ACCAAACGCCCCGAACA	GAGAGCTGCCACTTTGACGT
r p21/CIP1	CAGCCACAGGCACCATGTC	ACAGACGACGGCATACTTTGC
r p53	CTGGACGACAGGCAGACTTT	GCACAAACACGAACCTCAAA
r p27	CCGCCTGCAGAAACCTCTT	TCGGCAGTGCTTCTCCAAGT
r p19	ACCCCAAGTGAGGGTTTTCT	GATCCTCTCTGGCCTCAACA

Primers for qPCR (Mouse primers)

Target	**Forward primer**	**Reverse primer**
mKdm3a-1	CCAGGAGAAGACTTCAGAGACATG	GGTGTACTCAGGCAGTGGAATG
mKdm3a-2	TCTCTCTCAGTGTCCAGCTTTGAA	CGTGAGCACCATGGTTTCC
mKdm4c	CCATTCATCCACACCCTCAT	TTGGAACGCAAATACTGGAA
mCenpa	TTCTGTCTTCTGCGCAGTGT	GACCCCAAGGAGGAGACC
mNcapd2	AACCTGCAGTACCATCTCGG	CATGTGCATTCTGCTAGACCA
mNcapg2	CGGTGGTTTTGTCATGGATT	TGGAGATCACTTTGGAAGAGG
mCenpp	GGGAACAGGTACCCTCCAAG	TGTGGAGTGGTGTGAATATCG
mCenpi	TACAGCGACAACAAAGCCTG	GGAGAATGTCAAACCATTTCG
mCenpb	TGAATTCAAGCTGGGAAAGG	CTACAGGCCTCTGCCTCATC
mNcaph	AAGAACATCCTGTTGTCCTCG	TGGGCGCGATTTAAAACTTA
mSmc4	ATGTTCAGTCTGGCCTTTGG	GAAGCCATGGCATTGACTTAG
mSmc2	GCCATGCAGTCCATCTGTTA	AACCAAGCGCAAAGAGCTAC
mp21	GTGTGCCGTTGTCTCTTC	AATCTTCAGGCCGCTCAG
mp53	CGACCTATCCTTACCATCATC	AACTCTAAGGCCTCATTCAGC
mBax	GGAGCAGCTTGGGAGCG	AAAAGGCCCCTGTCTTCATGA
mGADD34	CCCGAGATTCCTCTAAAAGC	CCAGACAGCAAGGAAATGG
mSuv39H1	GCTCTGCCTCCTCTGAGGTAA	TCTCTGCATCTTCCGCACTA

mCenpu	ATCTGTGTCTGTGTGTCCGC	AGACACCAGCAACCCAAAGT
mHjurp	CAGAGGCTTCTCTCATCGCT	TTAAATGGGCAAGCTCCAGA

Primers for ChIP

Target	**Forward primer**	**Reverse primer**
h5S Ribosomal DNA (Chen et al., 2014)	ACGCTGGGTTCCCTGCCGTT	TGGCTGGCGTCTGTGGCACCCGCT
hSatellite 2 (Chen et al., 2014)	TCGCATAGAATCGAATGGAA	GCATTCGAGTCCGTGGA
hD4Z4 (Chen et al., 2014)	CAGGCCTCCTGGCTGCACCT	TGAGCCCCGGCCGGAA TTTCA
h17 alphoid (Chen et al., 2014)	CAACTCCCAGAGTTTCACA TTGC	GGAAACTGCTCTTTGAAAAGGAACC
h21-I alphoid a (Chen et al., 2014)	CTAGACAGAAGCCCTCTCAG	GGGAAGACA TTCCCTTTTTCACC
h21-I alphoid b (Chen et al., 2014)	GTAGTTTGTGGAAGTGGAC	CTGAGAATGCTGCTGTCTACC
hX alphoid a (Chen et al., 2014)	AGA TTTGGACCGCTTTGAGGC	CCGTTCAGTTATGGGAAGTTGA
hX alphoid b (Chen et al., 2014)	CCACAGAAAAACTAAACTGAAGC	GGCTTTCAGGCCTTTTCCACCAC
p15 promoter (Feng et al., 2014)	CTGCCTGGGGATGAATTTAAC	GGTTTCACTGTGGAGACGTTG
p21 promoter (Ohzeki et al., 2012)	TGTGTCCTCCTGGAGAGTGC	CAGTCCCTCGCCTGCGTTG
LMNB1 promoter (Piva et al., 2015)	GTCACCCTCGTCTTGCATTT	GCGTTTAGAGGAACGGAGAA
CENPA promoter (Sidler et al., 2014)	CCTTGGTGTTATGCTCTGGGAAG	GGGCTGTTACTGTTTTCTCAGGTTG
SUV39H1 promoter (Wang et al., 2016)	GCAACTTGAGGACGTGACAG	CCAGCTGTGATTCCTGACAA
KDM3A promoter (Wang et al., 2005)	CTTTCCTGTGAGATTCTTCCGCCA	CCGCGAAATCGGTTATCAACTTTGGG
KDM4C promoter (Wang et al., 2005)	TCCTTCTACGCGAGTATCTTTCCC	GTCACGTGGGCTTACAAACAGCTT

Supplementary Table S3. Antibodies used in this study, Related to Figure 1 to Figure 7

Antibody name	Company	Catalogue number	Isotype
Mono-Methyl-Histone H3 (Lys9) (D1P5R) Rabbit mAb	Cell Signaling Technology	14186	Rabbit
Di-Methyl-Histone H3 (Lys9) (D85B4) XP/TM Rabbit mAb	Cell Signaling Technology	4658	Rabbit
Tri-Methyl-Histone H3 (Lys9) (D4W1U) Rabbit mAb	Cell Signaling Technology	13969	Rabbit
Di/Tri-Methyl-Histone H3 (Lys9) (6F12) Mouse mAb	Cell Signaling Technology	5327	Mouse
Pan-Methyl-Histone H3 (Lys9) (D54) XP Rabbit mAb	Cell Signaling Technology	4473	Rabbit
Histone H3 (D1H2) XP Rabbit mAb	Cell Signaling Technology	4499	Rabbit
Phospho-Histone H2A.X (Ser139) Antibody	Cell Signaling Technology	2577	Rabbit
53BP1 Antibody	Novus	NB100-304	Rabbit
p21 Waf1/Cip1 (DCS60) Mouse mAb	Cell Signaling Technology	2946	Mouse
p21 (F-5)	Santa Cruz Biotechnology	sc-6246	Mouse
p53 (N-19)	Santa Cruz Biotechnology	sc-1314	Goat
p53 (1C12) Mouse mAb	Cell Signaling Technology	2524	Mouse
Lamin A/C (H-110)	Santa Cruz Biotechnology	sc-20681	Rabbit
p15 (C-20)	Santa Cruz Biotechnology	sc-612	Rabbit
HP1γ	Cell Signaling Technology	2619	Rabbit

Phospho-mTOR (Ser2448)	Cell Signaling Technology	5536	Rabbit
Phospho-Rb (Ser807/811) Antibody	Cell Signaling Technology	9308	Rabbit
Rb (4H1) Mouse mAb	Cell Signaling Technology	9309	Mouse
Lamin B1	abcam	ab16048	Rabbit
PCNA (PC-10)	Santa Cruz Biotechnology	sc-56	Mouse
β-tubulin monoclonal antobody	ImmunoWay Biotechnology	YM3139	Mouse
β Tubulin (H-235)	Santa Cruz Biotechnology	sc-9104	Rabbit
Anti-β-Actin mouse mAb	Sigma	A1978	Mouse
β-Actin (D6A8) Rabbit mAb	Cell Signaling Technology	8457	Rabbit
KDM3A (T-14)	Santa Cruz Biotechnology	sc-107656	Goat
KDM3A Polyclonal anitbody	Proteintech	12835-1-AP	Rabbit
Anti-KDM3A / JHDM2A antibody [14F8]	abcam	ab91252	Mouse
Anti-JMJD1A antibody	abcam	ab106456	Rabbit
KDM4C antibody	Bethyl	A300-885A	Rabbit
KDM4C polyclonal antibody	Novus	NBP1-49600	Rabbit
Anti-SUV39H1, clone MG44	Merck Millipore	05-615	Mouse
Anti-KMT1A/SUV39H1antibody	abcam	ab155164	Rabbit
Anti-CENPA antibody [3-19]	abcam	ab13939	Mouse
Anti-HJURP, clone 144K/B1	Merck Millipore	MABE441	Mouse
NCAPD2 Polyclonal antibody	Proteintech	13382-1AP	Rabbit
Anti-NCAPG2 antibody	abcam	ab70350	Rabbit

Transparent Methods

Isolation and characterization of MSCs

The use of human bone marrow and human umbilical cord for MSC isolation were approved by Joint CUHK-NTEC Clinical Research Ethics Committee (ethical approval code: CRE-2011.383, CRE-2010.248 and CRE-2015.018). Clinical specimens were collected in operation theatre, transported to clean room (ISO Class 7; Certified by NEBB) and immersed in Dulbecco's Phosphate Buffered Saline (DPBS) containing 10% P/S during removal of surrounding tissues/muscles/vessels under dissecting microscope (Nikon). The tissues were washed with DPBS twice thoroughly and cut into small pieces and cultured in Knockout DMEM (KO-DMEM, Cell Treatment Therapy, CTS, grade) supplemented with 10% FBS, 1% P/S (CTS) and 1% glutamax (CTS). For the adult bone marrow aspirate, MSCs were isolated by gradient centrifugation in Ficoll®-Paque PREMIUM 1.073 (GE Healthcare, Chicago, Illinois). The mononuclear cells were cultured in α-MEM supplemented with 10% FBS and 1% P/S. At confluence, the cells were trypsinized by TrypLE (CTS), and subjected to either passaging or cryopreserved in 5% DMSO (Sigma Aldrich, 30% FBS, 5% DMSO and 65% KO-DMEM) freezing medium. These MSCs were characterized according to ISCT (2006) minimal criteria. Reagents for cell culture were purchased from Gibco, Life Technologies. Unless otherwise specified, all chemicals were purchased from Sigma-Aldrich. Three hUCMSCs lines (hUC009, hUC011, hUC013) and three hBMSCs lines (hBM001, hBM003, hBM005) were used for functional study. BMSCs derived from nine young (13- to 35-year-old) and five old (52- to 61-year-old) individuals at passage 3 were collected for western blot analyzing the protein expression of senescence markers. Detailed information of this batch of BMSCs is shown in supplementary Table S1.

For primary rat BMSCs isolation, BM was harvested and pooled by flushing the tibias and femurs of rats with α-MEM supplemented with 10% FBS and 1% penicillin-streptomycin in 50ml tubes, and centrifuged at 1500rpm for 5mins. Then cell pellets were re-suspended and cultured in 75 mm^2 flask with complete α-MEM. Medium was changed after 24h and 48h, and adherent cells were expanded after 4 days when cells reached 80%-90% confluence. Phenotype analysis of surface markers was done at passage 2 based on two positive markers CD90, CD54 and two negative markers CD45 and CD34 by FACS. Mouse BMSCs were isolated from bone marrow and compact bone, and the detailed protocols were described previously (Soleimani and Nadri, 2009; Zhu et al., 2010). Compact bone pieces were seeded into 24-well plates and mouse BMSCs derived from compact bone pieces were used for immunofluorescence staining and western blot. Mouse BMSCs collected from bone marrow were used for RNA extraction and real time PCR.

Cell treatment in vitro

To establish replicative senescence model, primary human UCMSCs (Passage 3) or BMSCs (Passage 3) were passaged when cells were grown to 90% confluence. The cells were split in 1:3 and then collected at different passage numbers for cell functional analyses and biochemical analyses. To establish DNA damage-induced cellular senescence, early passage hUCMSCs (p6-p8) were treated with Doxorubicin (Selleckchem, Houston, TX, USA) at 5×10^{-8}M. Samples were treated with Doxorubicin for indicated time points and collected at 0, 3, 7, 10, 12, 24, 36 and 48h for Western blot and Immunofluorescence staining. For IOX1 treatment, hUCMSCs at p6-p8 were treated with IOX1 (Selleckchem, Houston, TX, USA) at different concentrations (20, 50, 70, 100μM) for 3 days, and then harvested for MTT, Western blot, qPCR assay and

β-Gal staining. For ChIP-qPCR assay, hUCMSCs at passage 6-8 were treated with IOX1 at the concentration of 70μM for 1 day, and then fixed with 1% formaldehyde and harvested for ChIP-qPCR assay. For IOX1 treatment during DOX-induced DNA damage, hUCMSCs at p6-p8 were pre-treated with IOX1 (50μM) for 2 days, treated with Doxorubicin at 5×10^{-8} M for 10 hours, and then harvested for Immunofluorescence staining.

β-Gal Staining

We used a β-Gal Staining assay kit (Cell Signaling Technology, Danvers, MA, USA) following the manufacturer's protocol. Briefly, cells were washed with PBS twice and fixed with 1 × Fixative Solution for 10 min at room temperature. After washing, the cells were incubated at 37°C with fresh β-Galactosidase Staining Solution [pH 6.0]. The experiment was repeated three times and the number of cells expressing β-Gal was calculated.

Clonogenic assay

2000 cells were seeded in 60 × 15mm cell culture dish, and cultured for continuous 10 days. After that, cells were fixed with cooled absolute methanol for 2 minutes and stained for 5 minutes with 1% crystal violet aqueous solution.

siRNA-mediated knockdown and plasmid transfection

siRNA pools targeting KDM3A and KDM4C were purchased from Invitrogen (Life Technologies, Carlsbad, USA). KDM3A, KDM4C and NCAPD2 plasmids (pcDNA3.1(+)-KDM3A, pcDNA3.1(+)-KDM4C and pcDNA3.1(+)-NCAPD2) were purchased from Viral therapy Technologies Co. Ltd (Wuhan, China). hUCMSCs (p6-

p8) were transfected with siRNAs or plasmids using Lipofectamine® 2000 Transfection Reagent (Life Technologies). 48 - 72 hours after transfection, knockdown or overexpression efficiency were determined by quantitative real-time PCR or Western blot, and other molecular analyses including RNA-seq analyses, detection of downstream targets and ChIP assays. siRNAs used in this study are: KDM3A siRNA ID: HSS125107, HSS125109, HSS183294; KDM4C siRNA ID: HSS118146, HSS177158, HSS177159. For cell functional analyses, early passage hUCMSCs (P6-8) were pre-treated with siRNAs mixture (siKDM3A and siKDM4C) or scrambled siRNA for two days, and then treated with Doxorubicin at 5×10^{-8} M for 12 hours. Samples were then collected for immunofluorescent staining and β-Gal staining. For overexpression experiments, early passage hUCMSCs (p6-8) were transfected with KDM3A, KDM4C or NCAPD2 or control vectors for 24 hours, and then treated with medium containing 5×10^{-8}M Doxorubicin for another 12 hours.

Lentiviral shRNA knockdown

Stable knockdown of KDM3A or KDM4C cells was achieved by lentiviral transduction of pLVX- ShRNA-Puro-ZsGreen-hKDM3A-1, 2, 3 or pLVX-ShRNA-Puro-ZsGreen-hKDM4C-1, 2, 3 (Viraltherapy Technologies, Wuhan, China) or control virus pLVX- ShRNA-Puro-ZsGreen. After 48 h transduction, the transduced cells were propagated for two continuous passages, and then sorted by Flow Cytometer (BD FACSAria II Cell sorter) to select out positively-transduced cells based on ZsGreen positivity. shRNA targeting sequences are shown below: shKDM3A-1：5‘- CCT CCG GAA TCT CTT GAA TTC TTC T-3’; shKDM3A-2：5‘- GCA GCT GTA CTC AGC CTA AGA-3’; shKDM3A-3：5‘- GCA GGT GTC AAT AGT GAT AGC-3’; shKDM4C-1：5‘-GAG GAG TTC CGG GAG TTC AAC AAA T-3’; shKDM4C-2：

5‘- GGA GTT CAA CAA ATA CCT TGC-3’; shKDM4C-3：5‘- GCA GGT GGA GCA GAA TTT ATC-3’.

Real-time Reverse Transcriptase-Polymerase Chain Reaction (qRT-PCR)

Total RNA was isolated from MSCs using Trizol reagent (Life Technologies). 2 μg RNA was used to synthesize cDNA with oligo (dT) and reverse transcriptase, following the manufacturer’s protocol (Promega, Madison, WI, USA). Real-time RT-PCR reactions were performed using the SYBR Green PCR kit (Takara, Kusatsu, Shiga, Japan) and a 7500 Fast Real-Time PCR System (Applied Biosystems, CA, USA). The primers used for specific genes is presented in Supplementary Table S2.

RNA-Seq and Data processing

The construction of RNA-seq library and the sequencing were done by Beijing Genomics Institute (Shenzhen, China). Briefly, total RNA from treated samples was extracted using Trizol reagent (Life Technologies, Carlsbad, CA, USA). mRNA samples were prepared for RNA-Seq analysis using the Illumina TruSeq RNA Sample Prep Kit V2 (Illumina, San Diego, CA) according to the manufacturer's protocol. To produce the final cDNA libraries, universal adapters were ligated to the cDNA fragments followed by PCR amplification. The quality of sequencing library was tested using Agilent 2100 bioanalyzer. For enrichment of cDNA in the library, polymerase chain reaction (PCR) was carried out which selectively amplified those fragments with adapter molecules on both ends. The established cDNA libraries were applied to HiSeq2000 platform (TruSeq SBS KIT-HS V3, Illumina) with paired-end sequencing length of 90 bp. The levels of gene expression level and the differentially expressed genes were analyzed using the method described by Audic and Claverie(Audic and

Claverie, 1997). Levels of gene expression were calculated using the reads per kilobase million (RPKM) method. In cases where more than one transcript was found for a gene, the longest read was used to calculate its expression level and coverage. The significantly differentially expressed genes (DEG) were determined at a threshold false discovery rate (FDR) ≤ 0.05 and the absolute value of log2ratio ≥ 1 or ≤ 1. All DEGs were mapped to GO terms in the database (http://www.geneontology.org/); gene numbers have been calculated for every term, using a hypergeometric distribution compared with the genome background. We used Partek software to conduct GO analysis and mapped all the DEGs obtained from these libraries (p value < 0.05) to GO database, to classify for enriched GO terms, and analyze the DEGs based on the Organelle organization and Chromosome organization. Genomic data generated during the study are available in a public repository GEO (GSE133098).

Western Blot Analysis

Cells were lysed and protein was extracted using RIPA (Pierce, Rockford, IL, USA) plus protease inhibitor cocktail (Thermo Fisher, Waltham, MA, USA), and protein concentrations were determined using the BCA assay (Bio-Rad, Richmond, CA, USA). Aliquots of protein lysates were separated on SDS-6, 8, 10, 12% polyacrylamide gels and transferred onto polyvinylidene difluoride (PVDF) membrane, which was blocked with 4% blotting-grade milk in TBST (20 mM Tris–HCl [pH 7.6], 137 mM NaCl, and 1% Tween 20). The membrane was then hybridized with the indicated primary antibodies followed by the corresponding secondary antibodies, and then detected using ECL (GE). Membranes were exposed to X-ray film (Fuji Photo Film, Tokyo, Japan) to visualize the bands. The antibodies used in this study are listed in Supplementary Table S3.

Chromatin immunoprecipitation (ChIP) assay

We used a ChIP assay kit (Merck Millipore, Darmstadt, Germany) following the manufacturer's protocol. Briefly, cells were incubated with 1% formaldehyde (Sigma-Aldrich, MO, USA) for 10 minutes at 37°C, and then quenched of formaldehyde using 2.5M glycine. Each ChIP reaction was performed using 6.0×10^6 cells. For DNA precipitation, we added 3-5 μg ChIP-grade antibodies against H3K9me1, H3K9me2, H3K9me3, KDM3A and KDM4C. The precipitated DNA samples were quantified by qPCR with primers targeting on special sites. Primers for ChIP assay are presented in Supplementary Table S2.

Immunofluorescence staining

Cells seeded on slides were fixed in 4% paraformaldehyde for 10 min, and were washed with PBS for three times. The immunofluorescence staining in detail was performed as previously described(Huang et al., 2016). The antibodies used for immunofluorescence staining were listed in Supplementary Table S2. The Alexa FluorSeries from Invitrogen were used as secondary antibodies. Images were taken using a confocal system with inverted microscope (Olympus FV1000) and analyzed with FluoView 4.2a. For all quantitative analyses, images were collected using the same acquisition parameters to facilitate fluorescence intensity comparisons between groups. Corrected total cell fluorescence intensity (CTCF) was defined as area × (mean intensity−background intensity). For DNA damage foci analysis, all experiments were repeated three times, each experiment were set up for triplicates. 5 fields per slide were analyzed under the microscope and no less than 100 cells were analyzed for quantification data.

Transmission electron microscopy (TEM)

hUCMSCs transfected with KDM3A or KDM4C plasmids after 24h were harvested, then fixed and processed for TEM, as described previously(Stolz et al., 1999). After dehydration, thin sections (70 nm) (Leica UCT7) were stained with uranyl acetate and lead citrate for observation under a Transmission Electron Microscope (Hitachi H-7700).

The establishment of Ovariectomized (OVX) rat model and isolation of rat BMSCs from OVX rat bone marrow

All animals were provided by the Laboratory Animal Service Center of the Chinese University of Hong Kong. They were maintained in an air-conditioned room with controlled temperature of 24 ± 2 °C and humidity of 55 ± 15%, in a 12 h light/darkness cycle regulation and were fed laboratory chow and water *ad libitum*. All animal experiments were conducted in accordance with the University Laboratory Animals Service Center's guidelines on animal experimentation with approval from the Animal Ethnics Committee of the University. Thirty 6 month-old Spraque-Dawley female rats were used. 24 rats were subject to ovariectomy, and 6 received sham surgery. Briefly, a 1.5 cm skin incision was made to expose the dorsolateral abdominal muscles and ligation was performed at the distal uterine horn to remove the ovarian tissue completely. 6 animals with sham surgery were sacrificed at week 0. 6 animals per group in the OVX treatment were euthanized at week 3, 6, 9 and 12 post-surgeries. Serum, uterus, body weight, lumber vertebra, femur, and tibia were collected at the time of euthanization, and the 5th lumbar vertebras (LV5) were dissected for measurement of trabecular micro-CT analysis. For primary rat BMSCs isolation, BM was harvested and

pooled by flushing the tibias and femurs of sham and OVX female rats (n = 6 for every group) and cultured in α-MEM supplemented with 10 % FBS, Glutamax (2 mg/ml) and 1 % penicillin-streptomycin. Medium was changed after 24h and 48h, and adherent cells were expanded after 4 days. Phenotype analysis of surface markers was done at passage 2 based on two positive markers CD90, CD54 and two negative markers CD45 and CD34 by FACS. Cells at passage 3 were used for western blot and qPCR assay.

Micro-computed Tomography (micro-CT) Scanning

The OVX rats LV5s and mouse femurs were scanned using a desktop preclinical specimen micro-CT (uCT-35, Scanco Medical, Bassersdorf, Switzerland). Briefly, the vertebral bodies or femurs were aligned perpendicularly to the scanning axis for a total scanning length of 6.0 mm at custom isotropic resolution of 8-µm isometric voxel size with a voltage of 70 kV p and a current of 114 µA. Three-dimensional (3D) reconstructions of mineralized tissues were performed by an application of a global threshold (211 mg hydroxyapatite/cm3), and a Gaussian filter (sigma = 0.8, support = 2) was used to suppress noise. A volume of interest (VOI) containing only trabecular bone within the vertebral body extracted from the cortical bone with 1.80-mm thick (150 slices) was acquired from both cranial and caudal growth plate-metaphyseal junctions. The three-dimensional reconstructed images were used directly to quantify microarchitecture, and the morphometric parameters including bone volume fraction (BV/TV), trabecular number (Tb.N, 1/mm) and trabecular separation (Tb.Sp, mm) were calculated with the image analysis program of the micro- CT workstation (Image Processing Language v4.29d, Scanco Medical, Switzerland)

Kdm3a$^{-/-}$ knockout mice

The *Kdm3a*$^{-/-}$ mice was created by Prof. Xu Jianming's lab at the Baylor College of Medicine, Houston, TX (Liu et al., 2010). Bone tissues were derived as described before for CT scanning and western blot analysis. BMSCs were derived from 6 month-old female WT (n=3) and *Kdm3a*$^{-/-}$ knockout mice (n=3), and then subjected to 5×10^{-8} Doxorubicin. Samples were collected at different time points for real-time and immunofluorescence staining. For the rescue experiment, isolated BMSCs from WT (n=3) and *Kdm3a*$^{-/-}$ knockout mice (n=3) were subjected to 5×10^{-8} Doxorubicin treatment and simultaneously KDM3A plasmid transfection. Treated samples were collected at 0, 3, 7, and 10 hours after treatment for immunofluorescence staining and β-Gal staining.

Statistical analysis

Data are presented as mean ± SEM. At least three independent experiments were performed for each assay. Statistical differences were calculated with the two-tailed Student's t test when comparing two conditions. One-way ANOVA and Tukey's post hoc test were used when there were more than two groups. We used Wilcoxon/Mann-Whitney method when normal data distribution cannot be assured. Results were considered statistically significant at *P < 0.05, ** P < 0.01, *** P < 0.001 and **** for P < 0.0001.

Supplemental References:

Audic, S., and Claverie, J.M. (1997). The significance of digital gene expression profiles. Genome Res 7, 986-995.

Chen, X., Iliopoulos, D., Zhang, Q., Tang, Q., Greenblatt, M.B., Hatziapostolou, M., Lim, E., Tam, W.L., Ni, M., Chen, Y., et al. (2014). XBP1 promotes triple-negative breast cancer by controlling the HIF1alpha pathway. Nature 508, 103-107.

Feng, Y., Wu, H., Xu, Y., Zhang, Z., Liu, T., Lin, X., and Feng, X.H. (2014). Zinc finger protein 451 is a novel Smad corepressor in transforming growth factor-beta signaling. J Biol Chem 289, 2072-2083.

Huang, B., Cheng, X., Wang, H., Huang, W., Wang, D., Zhang, K., Zhang, H., Xue, Z., Da, Y., and Zhang, N. (2016). Mesenchymal stem cells and their secreted molecules predominantly ameliorate fulminant hepatic failure and chronic liver fibrosis in mice respectively. Journal of translational medicine 14, 1.

Liu, Z., Zhou, S., Liao, L., Chen, X., Meistrich, M., and Xu, J. (2010). Jmjd1a demethylase-regulated histone modification is essential for cAMP-response element modulator-regulated gene expression and spermatogenesis. J Biol Chem 285, 2758-2770.

Ohzeki, J., Bergmann, J.H., Kouprina, N., Noskov, V.N., Nakano, M., Kimura, H., Earnshaw, W.C., Larionov, V., and Masumoto, H. (2012). Breaking the HAC Barrier: histone H3K9 acetyl/methyl balance regulates CENP-A assembly. EMBO J 31, 2391-2402.

Piva, R., Lambertini, E., Manferdini, C., Capanni, C., Penolazzi, L., Gabusi, E., Paolella, F., Lolli, A., Angelozzi, M., Lattanzi, G., et al. (2015). Slug transcription factor and nuclear Lamin B1 are upregulated in osteoarthritic chondrocytes. Osteoarthritis Cartilage 23, 1226-1230.

Sidler, C., Li, D., Wang, B., Kovalchuk, I., and Kovalchuk, O. (2014). SUV39H1 downregulation induces deheterochromatinization of satellite regions and senescence after exposure to ionizing radiation. Front Genet 5, 411.

Soleimani, M., and Nadri, S. (2009). A protocol for isolation and culture of mesenchymal stem cells from mouse bone marrow. Nature protocols 4, 102-106.

Stolz, D.B., Ross, M.A., Salem, H.M., Mars, W.M., Michalopoulos, G.K., and Enomoto, K. (1999). Cationic colloidal silica membrane perturbation as a means of examining changes at the sinusoidal surface during liver regeneration. The American journal of pathology 155, 1487-1498.

Wang, G., Yu, Y., Sun, C., Liu, T., Liang, T., Zhan, L., Lin, X., and Feng, X.H. (2016). STAT3 selectively interacts with Smad3 to antagonize TGF-beta signalling. Oncogene 35, 4388-4398.

Wang, I.C., Chen, Y.J., Hughes, D., Petrovic, V., Major, M.L., Park, H.J., Tan, Y., Ackerson, T., and Costa, R.H. (2005). Forkhead box M1 regulates the transcriptional network of genes essential for mitotic progression and genes encoding the SCF (Skp2-Cks1) ubiquitin ligase. Mol Cell Biol 25, 10875-10894.

Zhu, H., Guo, Z.-K., Jiang, X.-X., Li, H., Wang, X.-Y., Yao, H.-Y., Zhang, Y., and Mao, N. (2010). A protocol for isolation and culture of mesenchymal stem cells from mouse compact bone. Nature protocols 5, 550-560.